Effect of Low Temperature Annealing on Microstructural and Optical Properties of $(BaTiO_3)_{0.84}(CeO_2)_{0.16}$ Thin Films

Z.H. Dughaish*

Physics Department, College of Science, Qassim University, P.O. 6644, Buraidah 51452, Saudi Arabia

(Received December 24, 2011; in final form October 11, 2012)

$(BaTiO_3)_{0.84}(CeO_2)_{0.16}$ thin films were prepared by electron beam evaporation method. X-ray diffraction and scanning electron microscopy revealed the amorphous structure for the as-prepared films. The thin films were annealed at temperatures: 200, 300, 400 and 500 °C for 1 h in air. Small and low intensity crystalline peaks were observed at annealing temperature of 200 °C for 1 h. The intensity and the number of the crystalline peaks were increased with increasing annealing temperature. Nanocrystals, of dimensions in the range 60–76 nm, were obtained when the annealing was performed at 500 °C. The indexed diffraction pattern of the annealed thin film revealed a monoclinic structure. A two-layer model was used to describe the experimental ellipsometric data. The Bruggeman effective medium approximation was used to describe the surface roughness layer and the Cauchy dispersion relation was used to describe the main $(BaTiO_3)_{0.84}(CeO_2)_{0.16}$ layer. The optical constants of the thin films over 300–1100 nm spectral range were measured. The optical band gap showed gradual decrease with the annealing temperature. The accurate determination of the optical constants of the thin films is very useful and should be taken into consideration in the design of devices using optical thin films technology.

DOI: 10.12693/APhysPolA.123.87

PACS: 68.55.−a, 77.55.F−, 78.20.Ci, 78.66.−w, 81.15.−z, 81.40.Ef, 81.70.Fy

1. Introduction

Barium titanate ($BaTiO_3$) has recently gained much attention due to its high dielectric constant, ferroelectric activity, spontaneous polarization and nonlinear optical properties in both active and passive electronic components [1–4]. The influences of transition metal oxides and rare-earth oxides dopants on properties of $BaTiO_3$ have been investigated in order to improve its properties and widen its applications [5, 6]. In particular, mixing $BaTiO_3$ with CeO_2 could produce superior properties. Jones and Jaatinen [7] stated that Ce:$BaTiO_3$ exhibit a light induced change in refractive index, and have potential uses in many areas of optical communications and circuitry. The results show that it is possible to obtain both intensity dependent absorption and transparency in Ce:$BaTiO_3$ at different wavelengths. Cernea et al. [8] observed that dielectric ceramics of Ce:$BaTiO_3$ present practical interest because addition of cerium decreases significantly the Curie temperature (T_C) of $BaTiO_3$. Issa et al. [9] and Dughaish and Issa [10] showed that addition of low concentrations less than 5 mol.% CeO_2 to $BaTiO_3$ lattice lowered T_C and the addition of 16 mol.% CeO_2 to $BaTiO_3$ smeared out T_C and changed the structure from tetragonal phase into cubic phase at room temperature. This guided us to choose this system for this study because it has electrical permittivity higher than that of pure barium titanate, and its crystal structure (cubic [9]) will not change during operation since there is no transition temperature (the addition of CeO_2 smeared out the transition temperature T_C [10]) and looks promising to have wide applications in electronics, optoelectronics, and gas sensing applications.

2. Experimental details

$(BaTiO_3)_{0.84}(CeO_2)_{0.16}$ system was prepared by mixing the appropriate quantities of high purity CeO_2 and $BaTiO_3$ by the usual ceramic method. The 16 mol.% batch was dry mixed in an agate ball mill for 1 h, calcined in platinum crucibles at 800 °C for 2 h. The calcined lumps were ground by a mortar and pestle, pressed at 4×10^7 kg m^{-2} into pellets of 1.2 cm in diameter and about 0.15 cm in thickness. The pellets were fired at 1360 °C in a muffle furnace for 2 h in air, and cooled down to room temperature inside the furnace.

The thin films of $(BaTiO_3)_{0.84}(CeO_2)_{0.16}$ were prepared by electron beam evaporation, since it gives a high deposition rate and good film quality, using high vacuum coating unit type Edward 306 A. The system was pumped down to a pressure of 5×10^{-6} mbar. $(BaTiO_3)_{0.84}(CeO_2)_{0.16}$ pellet was degassed prior the start of the evaporation process by heating in a vacuum chamber with an electron gun. The films were deposited on pre-cleaned microscopic glass slides and one side polished Si (100) substrates. The substrates were carefully cleaned by using acetone and distilled water. The substrates were rotating during the deposition. The source to substrate distance was 20 cm and the deposition rate was about 4 nm/s. Film thicknesses and the rate of evaporation were monitored with a quartz crystal monitor attached to the vacuum system.

The microstructural and optical properties of the e-beam evaporated $(BaTiO_3)_{0.84}(CeO_2)_{0.16}$ thin films were characterized by X-ray diffraction (XRD), scanning electron microscope (SEM), energy dispersive analysis of X-ray (EDAX) and spectroscopic ellipsometry (SE). The SEM, EDAX and the ellipsometric measurements were carried out for samples prepared on Si (100) and the XRD measurements were carried out on glass substrates. Investigations of the crystal structure were carried out

*e-mail: zhdalmas45@gmail.com

by a Shimadzu Diffractometer XRD 6000, Japan, with Cu K_{α_1} radiation ($\lambda = 1.54056$ Å). The data collection was performed by step-scan modes, in a 2θ range between 10° and 75° with step-size of 0.02° and step time of 0.6 s. Pure silicon ($\approx 99.9999\%$) was used as an internal standard.

The surface morphology and crystal structure of the films were characterized by SEM type JOEL model JSM--6380 LA (Japan). The chemical composition of the films was analyzed using energy dispersive analysis of X-ray (EDAX) unit attached to the SEM.

Variable angle spectroscopic ellipsometry (VASE) data for $(BaTiO_3)_{0.84}(CeO_2)_{0.16}$ films prepared on Si (100) were obtained using a PHE-102 variable angle spectroscopic ellipsometer (Angstrom Advanced Inc.) in the wavelength range 300–1100 nm. The data were obtained at angles of incidence of 70° and 75°. The instrument measures the complex ratio of the Fresnel reflection coefficients for p- and s-polarized light and reports the ratio in terms of the ellipsometric parameters Ψ and Δ defined by the equation

$$F = \tan(\Psi)\exp(\mathrm{i}\Delta) = \frac{\tilde{r}_p}{\tilde{r}_s}, \tag{1}$$

$\tilde{r}_p, \tilde{r}_s$ are the amplitude reflection coefficients for light polarized in the p- and s-planes of incidence, respectively. The data obtained from the ellipsometer were accurately modeled using the PHE-102 software package. Ellipsometric data Ψ and Δ for variable wavelengths were fitted in the optical model.

The $(BaTiO_3)_{1-0.16}(CeO_2)_{0.16}$ thin films were annealed at 200, 300, 400 and 500 °C in a muffle furnace for 1 h in air. XRD and VASE were used to characterize the films, before and after the annealing process, by following the previously mentioned procedures.

3. Results and discussion

3.1. EDAX, XRD, and SEM examinations

The results of the EDAX analysis for $(BaTiO_3)_{1-0.16}(CeO_2)_{0.16}$ grown on Si (100) substrates revealed that all the elements: Ba, Ti, Ce and O are present. Normalizing the atomic percentages to the Ti ratio gives the composition $Ba_{0.96}TiCe_{0.29}O_{5.37}$ for the as-prepared film which indicates a lower Ba content. This reduction in Ba has been previously reported [11, 12]. Upon annealing and within a precision of 2 at.%, the EDAX analysis does not reveal any obvious change in the chemical composition of the films.

The X-ray diffraction patterns, of the $(BaTiO_3)_{0.84}(CeO_2)_{0.16}$ thin films, annealed at different temperatures are shown in Fig. 1a–e. The X-ray diffraction pattern of the as-prepared film (see Fig. 1a) contains no peaks which imply the amorphous structure. Crystalline peak at 2θ of 24° is observed after annealing the film at 200 °C for 1 h (see Fig. 1b). The crystallization increased through the film as the annealing temperature is increased, Fig. 1c,d, and became clearer. From the JCDPS files, the diffraction peaks can be identified as monoclinic barium titanium oxide ($Ba_6Ti_7O_{40}$) (JCDPS card no. 77-1566). It is worth mentioning that the $BaTiO_3$ ceramic source had tetragonal phase of stoichiometric $BaTiO_3$ (figure is not shown). CeO_2 peaks are not found in XRD pattern, which imply that Ce atoms replace Ba in the monoclinic lattice or segregate to the non-crystalline regions in the grain boundaries. Fasasi et al. [13] observed a similar absence of ZnO in XRD pattern of ZnO-doped $BaTiO_3$ grown by laser ablation and annealed at 550 °C for 12 h.

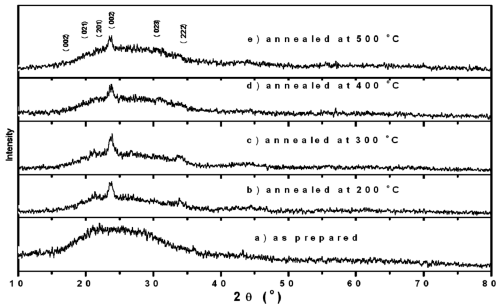

Fig. 1. XRD patterns of $(BaTiO_3)_{0.84}(CeO_2)_{0.16}$ thin films annealed at different temperatures.

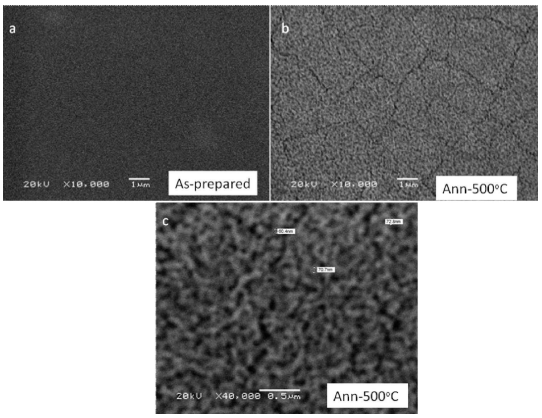

Fig. 2. SEM images of $(BaTiO_3)_{0.84}(CeO_2)_{0.16}$ thin films; (a) as-prepared; (b) and (c) low and high magnifications of the film annealed at 500 °C, respectively.

Figure 2a–c shows the SEM images of the as-prepared and annealed $(BaTiO_3)_{0.84}(CeO_2)_{0.16}$ thin films on Si (100) substrates. The micrograph of the as-prepared film (see Fig. 2a) shows a uniform film and smooth surface which confirms the amorphous structure. The film annealed at 500 °C shows obvious crystals with obvious grain boundaries (Fig. 2b and c). The obtained nanocrystals have dimensions in the range 60–76 nm (Fig. 2b).

3.2. Ellipsometric investigations

In order to estimate the optical constants of the $(BaTiO_3)_{0.84}(CeO_2)_{0.16}$ thin films, the ellipsometric spectra were analyzed by a multilayer modeling of a

two layer model (surface roughness layer and main $(BaTiO_3)_{0.84}(CeO_2)_{0.16}$ layer). The optical constants of Si obtained by Herzinger et al. [14] were used for the substrate. The complex refractive index of the surface roughness layer (SRL) was calculated by the Bruggeman effective medium approximation (BEMA) assuming a mixture of the "Lorenz oscillator-material" and a fitted percentage (volume fraction) of voids (air). The complex refractive index of the film was described by Cauchy model. The Cauchy dispersion relation can be expressed as

$$n(\lambda) = A_n + \frac{B_n}{\lambda^2} + \frac{C_n}{\lambda^4},$$

$$k(\lambda) = \alpha' \exp\left(B\left(\frac{1}{\lambda} - \frac{1}{\lambda_0}\right)\right). \tag{2}$$

The six parameters in this dispersion model are A_n, B_n, C_n, the extinction coefficient amplitude α', the exponent factor β, and the wavelength corresponding to the band gap value λ_0. All the Cauchy six parameters, the thickness and the voids fraction of the BEMA surface layer and the thickness of the interface layer were used as variable fit parameters. The fit to SE data at 70° and 75° incident angles were performed simultaneously. An example for the best fit of the experimental Ψ and Δ of the $(BaTiO_3)_{0.84}(CeO_2)_{0.16}$ films is shown in Fig. 3a and b. It is seen that there is a good agreement between the simulated and the measured data. Therefore, the optical constants can be adequately extracted. The presence of the interference patterns over the whole wavelength range is indicating that the films are transparent in the region. The thicknesses of the layers determined by VASE data fits are summarized in Table I. The surface roughness thickness is increased with increase of the annealing temperature. The thickness remains practically constant upon annealing at 200 °C. Annealing at 300 °C caused decrease in thickness. The increase in surface roughness and the decrease in thickness are associated with the crystallization [15].

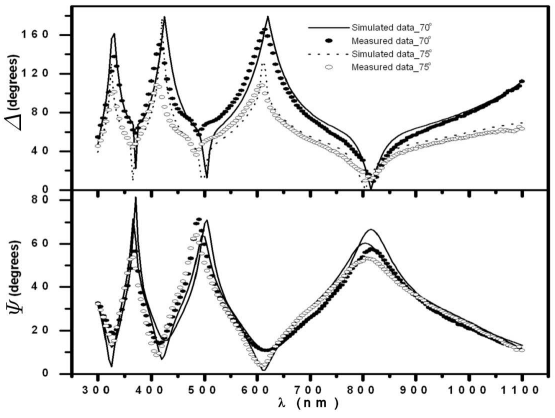

Fig. 3. Experimental and calculated ellipsometric parameters Ψ and Δ taken at angles of incidence 70° and 75°. The spectra are for the film annealed at 300 °C.

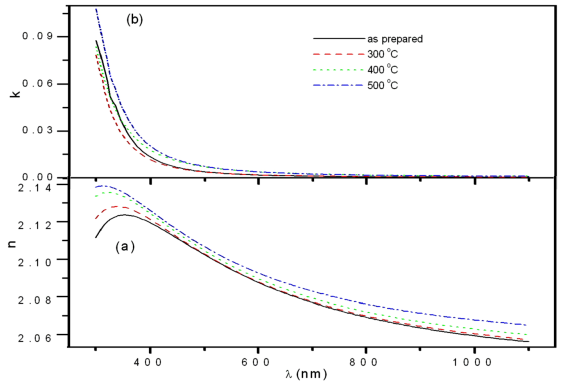

Fig. 4. (a) Refractive index n as a function of wavelength λ of $(BaTiO_3)_{0.84}(CeO_2)_{0.16}$ films annealed at different temperatures. (b) Extinction coefficient k as a function of wavelength λ of $(BaTiO_3)_{0.84}(CeO_2)_{0.16}$ films annealed at different temperatures.

TABLE I

Thickness derived from the ellipsometric data fitting (main/superficial layer) and optical band gap (E_g).

Annealing temperature [°C]	Thickness [nm] (main layer/SRL)	E_g [eV]
as-prepared	453.4/7.1	3.68
200	453.5/6.5	3.71
300	452.4/7.4	3.75
400	450.8/7.9	3.67
500	449.2/8.5	3.65

The obtained optical constants n and k of the $(BaTiO_3)_{0.84}(CeO_2)_{0.16}$ are shown in Fig. 4a and b, respectively. The refractive index follows a normal dispersion behavior with wavelength where it decreases as the wavelength increases. The refractive index n increases with increase of the annealing temperature. This can be ascribed, as previously reported for other oxides, to the increase in the density with increasing annealing temperature [15]. The extinction coefficient k values of the $(BaTiO_3)_{0.84}(CeO_2)_{0.16}$ films, annealed at different temperatures, are close to zero over most of the studied wavelength range, and increases rapidly at the short wavelengths (below 420 nm). The k-values increase as the annealing temperature increases. This may be related to the increase in surface roughness with increasing annealing temperature. The numerical values of our results for n and k agree with the results of Gao et al. [16] for BTO + 2 mol.% ZnO and 6 mol.% ZnO, Cai et al. [17], Wu et al. [18] for $Ba(Ti_{1-x}Ni_x)O_3$ thin films, and Filmetrics Tables, 2011 [19], at 400 nm and 700 nm wavelengths, Table II.

TABLE II
A comparison of the optical constants of $(BaTiO_3)_{0.84}(CeO_2)_{0.16}$ thin film with published data.

Material	k		n	
	λ (400 nm)	λ (700 nm)	λ (400 nm)	λ (700 nm)
$(BaTiO_3)_{0.84}(CeO_2)_{0.16}$ [present data]	0.015	0.0010	2.12	2.076
BTO + 2 mol.% ZnO, [16]	0.025	0.000	2.00	2.15
BTO + 6 mol.% ZnO, [16]	0.0135	0.000	1.98	2.00
BTO + 1 mol.% NiO_2, [17]	0.000			
BTO + 2 mol.% NiO_2, [17]	0.008			
BTO + 5 mol.% NiO_2, [17]	0.025			
BTO + 10 mol.% NiO_2, [17]	0.043			

The extinction coefficient k is related to the absorption coefficient α by the relation

$$\alpha = \frac{4\pi k}{\lambda}. \tag{3}$$

The optical band gap (E_g) values were calculated according to a direct allowed transition from the general relation $(\alpha\, h\nu) \propto (h\nu - E_g)^{1/2}$. The calculated E_g values are listed in Table III. It shows that E_g increases from 3.68 eV to 3.75 eV upon annealing at 300 °C. Annealing the films at temperatures above 300 °C leads to a continuous decrease in E_g values. The increase in E_g for the films annealed at 200 °C and 300 °C may be due to the reduction in defect centers (oxygen vacancies) as the stoichiometry improved upon oxidation. However, the decrease in E_g after the annealing at temperatures above 300 °C may be related to the structure transformation from amorphous to crystalline [20]. Our results for E_g agree with the results of Gao et al. [16] for BTO + 2 mol.% ZnO and 6 mol.% ZnO, Wu et al. [18] for $Ba(Ti_{1-x}Ni_x)O_3$ thin films, Cai et al. [17] and Filmetrics Tables, 2011 [19], at 400 nm and 700 nm wavelengths, Table III.

TABLE III
Comparison of the obtained E_g values with the published data.

Material	Annealing temp. [°C]	E_g [eV]
$(BaTiO_3)_{0.84}(CeO_2)_{0.16}$, [present data]	as-prepared	3.68
$(BaTiO_3)_{0.84}(CeO_2)_{0.16}$, [present data]	300	3.75
$(BaTiO_3)_{0.84}(CeO_2)_{0.16}$, [present data]	400	3.67
$(BaTiO_3)_{0.84}(CeO_2)_{0.16}$, [present data]	500	3.65
BTO pure, Ref. [18]	700	3.56
BTO pure, Ref. [18]	900	3.67
BTO + 1 mol.% NiO_2, Ref. [19]		3.58
BTO + 2 mol.% NiO_2, Ref. [19]		3.49
BTO + 5 mol.% NiO_2, Ref. [19]		3.35
BTO + 10 mol.% NiO_2, Ref. [19]		3.13

4. Conclusions

$(BaTiO_3)_{0.84}(CeO_2)_{0.16}$ thin films were prepared by e-beam evaporation and characterized by XRD, SEM, EDAX and SE. The XRD and SEM revealed the amorphous structure for the as-prepared films. Recrystallization was observed upon annealing the films at 200 °C in air for 1 h. The ellipsometric data from $(BaTiO_3)_{0.84}(CeO_2)_{0.16}$ thin films fit very well over a wide spectral range using a two-layer model. The thickness and optical constant were accurately determined with change in the annealing temperature. The refractive index showed a peak value when annealed at 300 °C, then dropped with further increase of the annealing temperature. The optical band gap showed gradual decrease with the annealing temperature. This accurate determination of the optical constants over a wide spectral range will be very useful and should be taken into consideration in designing devices using optical thin films technology.

Acknowledgments

Dr S.H. Mohamed and Prof. Dr. M. El-Hagary are acknowledged for their useful discussions and technical support. This work is supported by the Saudi Basic Industries Corporation (SABIC) and Deanship of Scientific Research at Qassim University, Saudi Arabia under the contract no. SR-S-010-10.

References

[1] C. Bi, M. Zhu, Q. Zhang, Y. Li, H. Wang, *Mater. Chem. Phys.* **126**, 596 (2011).

[2] D.A. Tenne, A. Soukiassian, X.X. Xi, H. Choosuwan, R. Guo, A.S. Bhalla, *Phys. Rev. B* **70**, 174302 (2004).

[3] A. Jezowski, J. Mucha, R. Pazik, W. Strek, *Appl. Phys. Lett.* **90**, 114104 (2007).

[4] Z.G. Hu, Y.W. Li, M. Zhu, Z.Q. Zhu, J.H. Chu, *Phys. Lett. A* **372**, 4521 (2008).

[5] S. Yoon, J. Dornseiffer, Y. Xiong, D. Grüner, Z. Shen, S. Iwaya, C. Pithan, R. Waser, *J. Eur. Ceram. Soc.* **31**, 773 (2011).

[6] A.Y. Fasasi, B.D. Ngomb, J.B. Kana-Kana, R. Bucher, M. Maaza, C. Theron, U. Buttner, *J. Phys. Chem. Solids* **70**, 1322 (2009).

[7] M.W. Jones, E. Jaatinen, *Opt. Mater.* **31**, 122 (2008).

[8] M. Cernea, O. Monnereau, P. Llewellyn, L. Tortet, C. Galassi, *J. Eur. Ceram. Soc.* **26**, 3241 (2006).

[9] A.A. Issa, N.M. Molokhia, Z.H. Dughaish, *J. Phys. D, Appl. Phys.* **16**, 1109 (1983).

[10] Z.H. Dughaish, A.A. Issa, *J. Nat. Sci. Math.* **2**, 63 (2008).

[11] S.-S. Park, J.-H. Ha, H.N. Wadley, *Integrat. Ferroelectr.* **95**, 251 (2007).

[12] S.H. Mohamed, Z.H. Dughaish, *Philos. Mag.* **92**, 1212 (2012).

[13] A.Y. Fasasi, M. Maaza, E.G. Rohwer, D. Knoessen, Ch. Theron, A. Leitch, U. Buttner, *Thin Solid Films* **516**, 6226 (2008).

[14] C.M. Herzinger, B. Johs, W.A. McGahan, J.A. Woollam, W. Paulson, *J. Appl. Phys.* **83**, 3323 (1998).

[15] S.H. Mohamed, O. Kappertz, T. Niemeier, R. Drese, M.M. Wakkad, M. Wuttig, *Thin Solid Films* **468**, 48 (2004).

[16] W.L. Gao, H.M. Deng, D.J. Huang, P.X. Yang, J.H. Chu, *J. Phys., Conf. Series* **276**, 012163 (2011).

[17] W. Cai, C. Fu, J. Gao, Q. Guo, X. Deng, C. Zhang, *Physica B* **406**, 3583 (2011).

[18] M. Wu, Z. Wang, T. Zhang, W.F. Zhang, *Thin Solid Films* **518**, 7007 (2010) .

[19] Filmetrics, 2011: `http://www.filmetrics.com/refractive-index-database/` .

[20] S.H. Mohamed, H.M. Ali, H.A. Mohamed, A.M. Salem, *Eur. Phys. J. Appl. Phys.* **31**, 95 (2005).